DmWRNexo is a 3′–5′ exonuclease: Phenotypic and biochemical characterization of mutants of the Drosophila orthologue of human WRN exonuclease

ARTICLE *in* BIOGERONTOLOGY · JUNE 2008

Impact Factor: 3.29 · DOI: 10.1007/s10522-008-9181-3

Biogerontology (2009) 10:267–277
DOI 10.1007/s10522-008-9181-3

RESEARCH ARTICLE

DmWRNexo is a 3′–5′ exonuclease: phenotypic and biochemical characterization of mutants of the *Drosophila* orthologue of human WRN exonuclease

Ivan Boubriak · Penelope A. Mason · David J. Clancy · Joel Dockray · Robert D. C. Saunders · Lynne S. Cox

Received: 3 September 2008 / Accepted: 25 September 2008 / Published online: 28 October 2008

Abstract The premature human ageing Werner's syndrome is caused by loss or mutation of the WRN helicase/exonuclease. We have recently identified the orthologue of the WRN exonuclease in flies, DmWRNexo, encoded by the *CG7670* locus, and showed very high levels of mitotic recombination in a hypomorphic PiggyBac insertional mutant. Here, we report a novel allele of *CG7670*, with a point mutation resulting in the change of the conserved aspartate (229) to valine. Flies bearing this mutation show levels of mitotic recombination 20-fold higher than wild type. Molecular modelling suggests that D229 lies towards the outside of the molecule distant from the nuclease active site. We have produced recombinant protein of the D229V mutant, assayed its nuclease activity in vitro, and compared activity with that of wild type DmWRNexo and a D162A E164A double active site mutant we have created. We show for the first time that DmWRNexo has 3′–5′ exonuclease activity and that mutation within the presumptive active site disrupts exonuclease activity. Furthermore, we show that the D229V mutant has very limited exonuclease activity in vitro. Using *Drosophila*, we can therefore analyse WRN exonuclease from enzyme activity in vitro through to fly phenotype, and show that loss of exonuclease activity contributes to genome instability.

Keywords Werner syndrome · WRN · Exonuclease · *CG7670* · Aging · Ageing · Recombination · *Drosophila* · DmWRNexo

Abbreviations

BSA	Bovine serum albumin
DTT	Dithiothreitol
ECL	Enhanced chemiluminescence
HRP	Horse radish peroxidase
IPTG	Isopropyl β-D-1-thiogalactopyranoside
PBS	Phosphate buffered saline
TILLING	Targeting Induced Local Lesions IN Genomes
WS	Werner syndrome
WRN	Protein mutated in Werner syndrome

Introduction

Cellular senescence was first described in cultured cells by Hayflick (1965). It is thought to arise as a consequence of various stress signals feeding into a signalling network that results in loss of proliferative capacity (reviewed in Cox and Faragher 2007). One important signal for onset of senescence is DNA damage, arising either from exposure to exogenous

I. Boubriak · P. A. Mason · J. Dockray · L. S. Cox (✉)
Department of Biochemistry, University of Oxford, South Parks Road, Oxford OX1 3QU, UK
e-mail: lynne.cox@bioch.ox.ac.uk

D. J. Clancy · R. D. C. Saunders
Department of Life Sciences, The Open University, Milton Keynes MK7 6AA, UK

genotoxic agents, or from endogenous sources such as telomere attrition or the presence of stalled replication forks (Cox and Faragher 2007). The WRN helicase/exonuclease is important in replication fork progression (Rodriguez-Lopez et al. 2002; Sidorova et al. 2008), probably acting to prevent the accumulation of recombinogenic intermediates at stalled forks (Rodriguez-Lopez et al. 2007) or to repair damage caused by replication fork arrest (Dhillon et al. 2007). WRN is indeed implicated in DNA recombination and DNA repair (reviewed by Cheng et al. 2007; Cox and Faragher 2007). WRN thus plays an important role in maintaining genome stability, and its loss contributes to premature cellular senescence (Salk et al. 1981; Faragher et al. 1993) and organismal ageing in the progeroid Werner syndrome (WS) (Yu et al. 1996, 1997). The importance of stress signalling in premature senescence in Werner's syndrome is evident from the finding that inhibition of the stress kinase p38MAPK restores normal proliferation characteristics to Werner syndrome fibroblasts (Davis et al. 2005).

In vertebrates, WRN possesses both exonuclease and helicase domains within the same polypeptide, whilst in *E. coli*, yeast and *Arabidopsis*, these activities are encoded on distinct polypeptides (e.g. RecQ helicase and RecJ nuclease in *E. coli*, Courcelle and Hanawalt 1999). In *Drosophila*, we have recently identified an orthologue of the exonuclease component of human WRN, DmWRNexo (Cox et al. 2007; Saunders et al. 2008), which allows us to investigate the role of the exonuclease component of WRN distinct from the helicase component, in a metazoan animal with distinct developmental stages. DmWRNexo is encoded by the *CG7670* locus. A strong hypomorphic piggyBac insertional allele, $CG7670^{e04496}$, results in very high levels of mitotic recombination, as observed using the recessive marker *mwh* in the adult fly wing blade (Saunders et al. 2008), suggesting that WRN exonuclease activity is important to maintain genomic stability. In order to investigate the effect on flies of subtle alterations in DmWRNexo activity, we have employed the technique of Targeting Induced Local Lesions IN Genomes (TILLING) (McCallum et al. 2000; Till et al. 2003) to identify a mutant allele of *CG7670*, bearing a point mutation in which the conserved aspartate 229 is altered to valine (D229V). We have analysed genome stability in $CG7670^{e04496}$/$CG7670^{D229V}$ flies and show moderately elevated levels of mitotic recombination. To investigate the molecular basis of this increased instability, we have also generated a recombinant version of DmWRNexo bearing the D229V mutation, and we compare its nuclease activity in vitro with both wild type recombinant DmWRNexo and a nuclease-dead mutant. This study allows us for the first time to relate the in vivo phenotype of flies mutant for WRN exonuclease to the in vitro biochemical activity of DmWRNexo.

Methods

Fly stocks and TILLING

Unless otherwise noted, fly stocks were obtained from the Bloomington *Drosophila* Stock Center (http://flystocks.bio.indiana.edu/), and were maintained on an oatmeal, yeast, cornmeal, dextrose, and agar medium at a constant temperature of 25°C. $CG7670^{e04496}$ bears a piggyBac insertion within the 5′ UTR, and is a strong hypomorph (Cox et al. 2007; Saunders et al. 2008). The $CG7670^{D229V}$ allele was identified through the Fly-TILL project (http://tilling.fhcrc.org:9366/fly/Welcome_to_Fly-TILL.html) (McCallum et al. 2000; Till et al. 2003). To analyze recombination as revealed through the *mwh* marker, adult wing blades were dissected from flies stored in 70% ethanol, mounted in Gary's Magic Mountant (Lawrence et al. 1986) and analysed by brightfield microscopy (Saunders et al. 2008).

Bioinformatics and molecular modelling

DmWRNexo structure was modelled by fitting to the PDB co-ordinates published for human WRN (2fby) (Perry et al. 2006) using Swiss Model (Peitsch et al. 1996; Schwede et al. 2003) then imported into PyMol v 0.99 (Delano Scientific). Residues were coloured and the image merged with human WRN exonuclease domain using PyMol software.

DNA preparation and site-directed mutagenesis

CG7670 DNA (Saunders et al. 2008) was subcloned into pIVEX2.3d (Roche) using restriction sites NdeI and SmaI, transformed into chemically competent

E. coli DH5α and DNA prepared by standard methods (Qiagen). Site directed mutagenesis to generate the D229V mutation was performed using the Stratagene Quikchange II kit according to manufacturer's instructions, with primers: forward 5′-GAAAGCTGGC ACGTGTTTTCCCCGAGGTTAC-3′ and reverse 5′-GTAACCTCGGGGAAAACACGTGCCAGCTTT C-3′, under the following PCR conditions: 95°C 30 s (1 cycle) then 16 cycles of 95°C 30 s, 55°C 60 s, 68°C 6 min 20 s, followed by digestion with DpnI for 90 min at 37°C and transformation into *E. coli* XL1-blue. Transformed bacteria were plated onto LB agar supplemented with 50 μg/ml ampicillin and grown inverted overnight at 37°C. DNA sequence analysis was performed on an ABI 3730xl DNA Analyser-Titania platform (GeneService, Department of Biochemistry, University of Oxford).

Recombinant protein expression and purification

For protein expression, the pIVEX2.3d vector with appropriate insert (or empty vector for negative controls) was transformed by heat shock into chemically competent *E. coli* BL21 T7 I^q LysY (NEB), grown in SOC medium for 30 min at 37°C 220 rpm then plated onto LB agar supplemented with ampicillin to 50 μg/ml and incubated overnight. Individual colonies were picked into 5 ml LB-amp and grown with shaking for 8 h at 37°C, then diluted 1:100 in fresh LB-amp and grown overnight at 37°C with shaking. Aliquots of this overnight culture were diluted 1:60 in a total volume of 1.8 litres of LB-amp, grown with shaking at 37°C for 3 h, induced by addition of 0.75 mM IPTG for 3.5 h, and then bacteria were harvested by centrifugation at 5,000 rpm 25 min 4°C in a Beckman JLA10 rotor. Medium was removed and the cell pellet frozen overnight at −80°C. Cells were lysed in buffer HS (250 mM NaCl, 5 mM DTT, 1 mM benzamidine, 0.5 mg/ml lysozyme) for 20 min on ice and supernatant harvested after centrifugation at 14,000 rpm 4°C in a Beckman GS-15R centrifuge rotor F3602.

Bacterial lysate was adjusted to 20 mM imidazole then applied to a 1 ml His-Trap column (GE Healthcare) and eluted over a step gradient of 40, 60, 100, 300 and 500 mM imidazole in PBS according to manufacturer's instructions (GE Healthcare). Column fractions were analysed by dot blotting. Briefly, 2 μl of each column fraction was spotted onto nitrocellulose, air dried then the membrane was blocked for 1 h room temperature with 5% non-fat milk in PBS with 0.2% Tween 20, washed and probed with HRP-conjugated anti-his monoclonal antibody (Roche) diluted 1:500 in 0.2% milk–PBS–Tween for 1 h at room temperature, then washed and the blot developed using the ECL system with exposure to Hyperfilm (GE Healthcare). Fractions were also analyzed on SDS-PAGE gels stained with Coomassie or silver, and by Western blotting using HRP-anti-his antibody (Roche). To confirm protein identity, major bands from peak fractions were excised from gels and subjected to *N* terminal sequencing (courtesy of Tony Willis, Protein sequencing facility, Department of Biochemistry, University of Oxford).

Nuclease assays

Recombinant proteins were desalted by passing through Sephadex G25 columns into buffer DS (150 mM Tris–HCl pH 8.0, 50 mM NaCl, 5 mM 2-mercaptoethanol, 0.1 × Complete EDTA-free protease inhibitors (Roche)), with the addition of glycerol to 20% before aliquotting and storage at −80°C. PAGE-purified fluorescein 5′ end-labelled 50-mer oligonucleotide (50-FLO in Table 1) and various complementary unlabelled oligonucleotides were obtained from Invitrogen and stored in 10 mM Tris–HCl pH 7.6 at 1 nmol/μl at −20°C and in the dark (see Table 1 for sequences). Duplex substrates were annealed as 1:1.2 (molar ratio) of fluorescent oligonucleotide: complementary oligonucleotide in 1 × TE with 50 mM NaCl, heated to 95°C for 3 min then allowed to cool slowly to below 30°C. Substrates were checked for annealing using non-denaturing SDS–PAGE. Working aliquots of annealed substrates were kept at 4°C.

Exonuclease assays were conducted using 1 pmol of recombinant DmWRNexo protein with 20 pmol oligonucleotide in WRN exo buffer [40 mM Tris–HCl, pH 8.0, 4 mM $MgCl_2$, 5 mM dithiothreitol, 0.1 mg/ml BSA (Opresko et al. 2001)] and incubated at 18, 25 or 37°C for up to 40 min. Reactions were stopped by the addition of formamide buffer [80% formamide, 0.5 × TBE ± bromophenol blue and xylene cyanol (Opresko et al. 2001)]. Products were resolved on 14% acrylamide gels containing 8 M urea at 200 V for 150–200 min. DNA fragments were visualized on a Fuji FLA-3000 with filter 470/520

Table 1 Oligonucleotides used in this study

(a) Name	Sequence 5′–3′
50-FLO	●GAACTATGGCTCTCGAGTGCTAGGACATGTCTGACTACGTACAAGTCACC
B-50	GGTGACTTGTACGTAGTCAGACATGTCCTAGCACTCGAGAGCCATAGTTC
RO-65-5′	$(T)_{15}$GGTGACTTGTACGTAGTCAGACATGTCCTAGCACTCGAGAGCCATAGTTC

(b) Name	Oligos used	Substrate characteristics
ssFLO	50-FLO	50
Blunt	50-FLO + B-50	50
5′ overhang	50-FLO + RO-65-5′	50 15

(a) Sequences of oligonucleotides. (b). Substrates for nuclease assays derived from the oligonucleotides shown in part (a). Filled circle denotes fluorescein label. Size in nucleotides is given below the substrate

and the most sensitive settings i.e. 16-bit imaging, F-1,000 and a resolution of 50. Quantitation utilised ImageJ (http://rsbweb.nih.gov/ij/index.html).

Results

We have recently shown that very low expression of DmWRNexo through piggyBac insertion in the 5′ UTR of *CG7670* leads to very high levels of DNA recombination, as assayed by the recessive multiple wing hairs marker (*mwh*) (Saunders et al. 2008). While cells heterozygous for *mwh* show the usual one hair per wing blade cell, cells that are either hemizygous or homozygous for *mwh* display tufts of wing hairs. To investigate what, if any, impact a milder mutation in DmWRNexo might have in genome stability, a fly stock bearing a point mutation altering aspartate 229 to valine was obtained by TILLING (see "Methods").

Recombination in $CG7670^{D229V}$ flies

To analyse if the $CG7670^{D229V}$ mutant allele has an impact on genomic stability, compound heterozygote flies with one copy of the D229V allele and one copy of the piggyBac allele (i.e. mwh^1 $CG7670^{e04496}$/$CG7670^{D229V}$) were scored for frequency and size of wing blade clones. Recombination rates were compared with those for flies homozygous for the piggyBac insertional allele (mwh^1 $CG7670^{e04496}$/$CG7670^{e04496}$) and flies hemizygous for $CG7670^{e04496}$ (mwh^1 $CG7670^{e04496}$/*Df(3R)Exel6178*). Interestingly, $CG7670^{e04496}$ hemizygotes (Fig. 1a) show approximately twice the rate of recombination (for single cell clones) as observed for $CG7670^{e04496}$ homozygotes (Fig. 1b), strongly suggesting that this allele is hypomorphic, and demonstrating a gene dosage effect. The phenotypes observed (see also Cox et al. 2007; Saunders et al. 2008) are therefore likely to be due to a limiting amount of DmWRNexo. By contrast, rates of recombination in mwh^1 $CG7670^{e04496}$/$CG7670^{D229V}$ flies were much lower (Fig. 1c), though ~20-fold more single cell clones were observed than in mwh^1 $CG7670^{e04496}$/$CG7670^{+}$ heterozygotes (0.2 single cell clones per fly, data not shown, see Saunders et al. 2008). Thus mutation of aspartate D229 to valine has a marked deleterious impact on the activity of DmWRNexo in restraining excessive mitotic recombination in flies. In terms of the recombination phenotype (Fig. 1d), we can derive

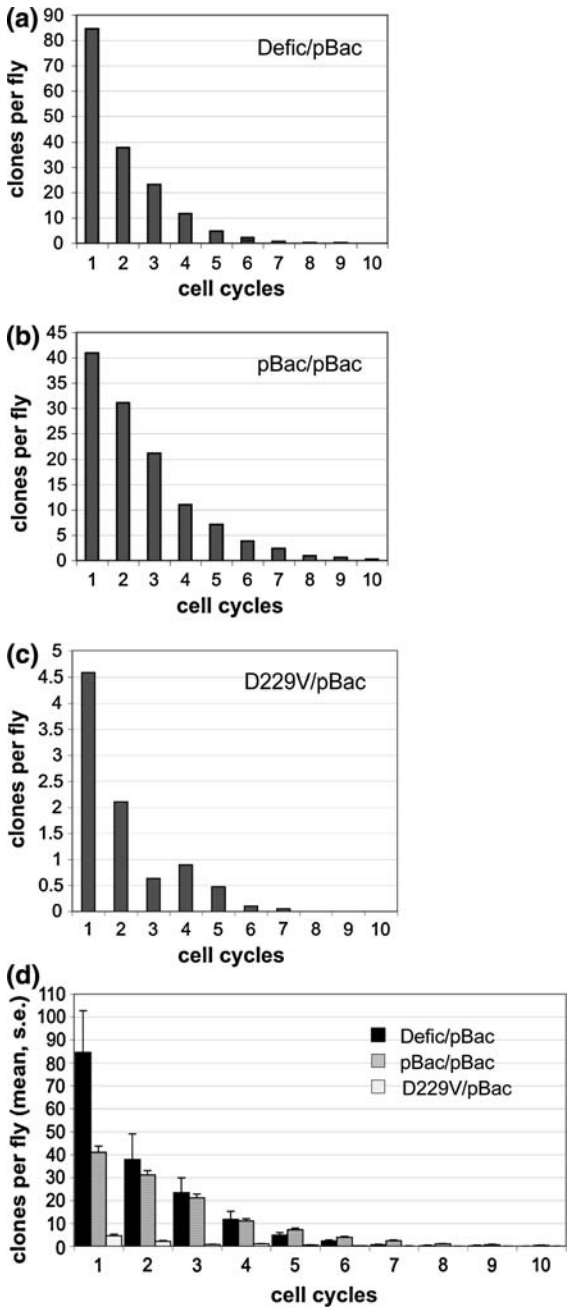

◀ **Fig. 1** Recombination frequencies in wing blades of flies bearing mutations in the gene for DmWRNexo. Recombination is determined by appearance of the multiple wing hair marker (observed as tufts of hairs in wing cells instead of the usual single wing blade hair per cell) and the frequency of such clones is plotted against the number of cell cycles since the recombination event, as determined from number of cells within the clone. Note that all flies are originally heterozygous for the recessive mwh marker: the clones of cells with scorable tufts of hair (i.e. homozygous for mwh^1) arise via mitotic recombination. **a** $CG7670^{e04496}$ hemizygotes mwh^1 $CG7670^{e04496}$/*Df (3R)Exel6178*, **b** $CG7670^{e04496}$ homozygotes mwh^1 $CG7670^{e04496}$/$CG7670^{e04496}$, **c** $CG7670^{D229V}$/mwh^1 $CG7670^{e04496}$. Note the different scales of the y axes in parts (**a**), (**b**) and (**c**). **d** Data from parts (**a**), (**b**) and (**c**) are combined to show the allelic series for severity of recombination phenotype

the allelic series: deficiency > $CG7670^{e04496}$ > $CG7670^{D229V}$. Note that even the relatively mild recombination phenotype seen in mwh^1 $CG7670^{e04496}$/$CG7670^{D229V}$ flies represents recombination rates more than 20-fold higher than levels observed in control flies, with a ~400-fold increase in recombination frequency in the $CG7670^{e04496}$ hemizygous flies over control flies.

Molecular modelling of the D229V mutation of DmWRNexo

To attempt to understand how the D229V mutation of DmWRNexo may impact on recombination and thereby result in the hyper-recombination phenotype, we modelled its position within the protein. A structural model of DmWRNexo was generated using Swiss Model and PyMol (coloured green in Fig. 2a, see also Saunders et al. 2008) according to the PDB co-ordinates of human WRN exonuclease domain (2fby, Perry et al. 2006, Fig. 2b). From this molecular modelling, it can be seen that the D229 residue (coloured yellow in DmWRNexo Fig. 2a, equivalent to D150 in human WRN, Fig. 2b) is not one of the acidic amino acids thought to be important for catalysis (D162, E164 and D222 in DmWRNexo, equivalent to D82, E84 and D143 in human WRN and coloured blue, magenta and red in Fig. 2, respectively), but instead lies spatially distant from the presumptive active site of the enzyme. The close fit of the model for DmWRNexo with respect to human WRN is shown in the merged structure (Fig. 2c).

Production of recombinant DmWRNexo protein

In order to investigate the molecular basis of the hyper-recombination detected in $CG7670^{e04496}$/$CG7670^{D229V}$ mutant flies, we generated the D229V mutant by site-directed mutagenesis of the wild-type clone (Saunders et al. 2008) in the vector pIVEX2.3d. We expressed a his-tagged recombinant version of the mutant $DmWRNexo^{D229V}$ in *E. coli*, in parallel

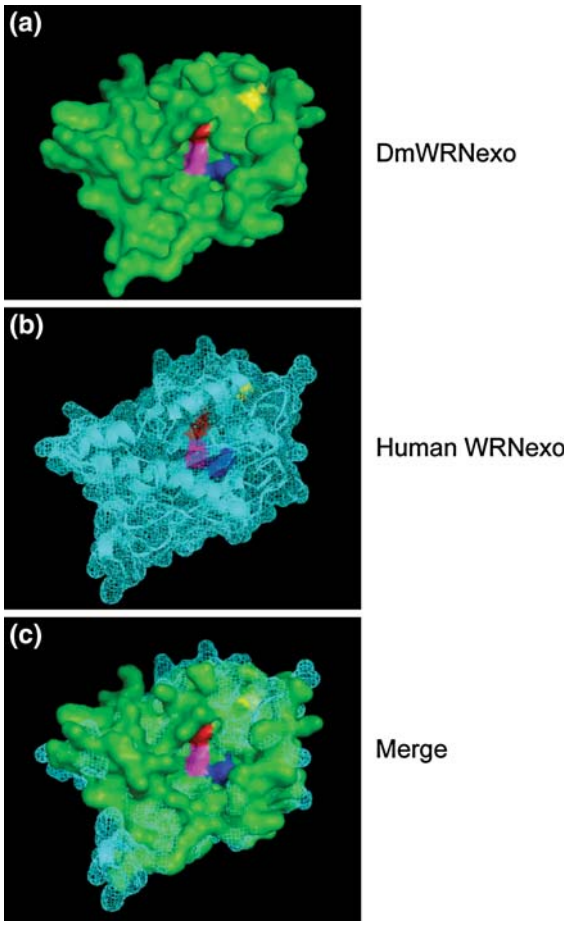

Fig. 2 Molecular modelling of DmWRNexo to show mutations generated **a** DmWRNexo predicted structure (see "Methods") is shown as a surface fill model, *in green*. **b** The structure of human WRN exonuclease domain as reported by Perry et al. (2006) is shown as a *cyan mesh*. **c** Merged structures of human and *Drosophila* WRN exonuclease. Individual residues are coloured as: *Blue*: *Drosophila* D162, equivalent to D82 (human); *Magenta* E164 (fly) E84 (human); *Red* D222 (fly) D143 (human); *Yellow* D229 (fly), D150 (human)

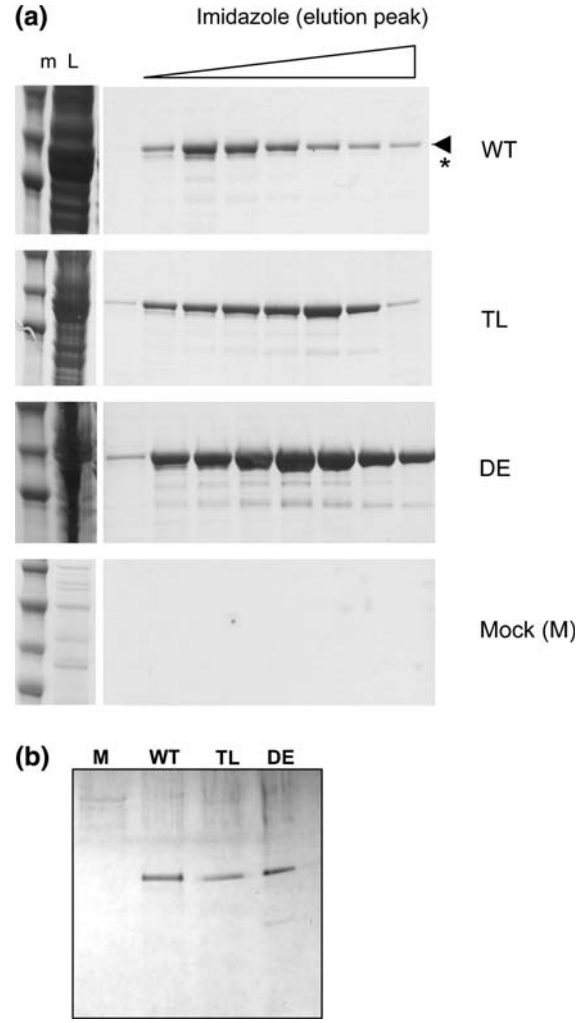

Fig. 3 DmWRNexo recombinant protein. **a** Coomassie-stained protein gels of peak fractions eluting between 300 and 500 mM imidazole for all purified recombinant proteins and the negative control. *m* = size marker, L = lysate. **b** Silver stained SDS-PAGE gel of desalted peak fractions used in subsequent nuclease assays. WT = wild type DmWRNexo, TL = DmWRNexo^{D229V} mutation ("TILLING"), DE = double mutant DmWRNexo^{D162A,E164A}, "M" = mock i.e. lysate from *E. coli* transformed with the empty vector

with wild type DmWRNexo and a double mutant form DmWRNexo^{D162A,E164A} in which presumptive active site residues (D162 and E164) are mutated to alanine, that we predict (see Fig. 2) should lack exonuclease activity. These proteins were purified by metal ion affinity chromatography. Peak fractions of his-tagged protein were found to elute between 300 and 500 mM imidazole from dot blot analysis (data not shown) and Coomassie-stained gels (Fig. 3a). For each peak fraction, following desalting, a major band of ~55 kDa representing purified recombinant DmWRNexo was observed on silver-stained SDS–PAGE (Fig. 3b). Western blotting was also performed using an antibody against hexa-histidine, confirming that the major Coomassie-stained DmWRNexo recombinant protein bands did indeed possess the expected histidine tag (data not shown). The identity of DmWRNexo was further confirmed by Edman degradation sequencing of excised bands; in addition to the major band for wt DmWRNexo, a

minor band of 51kDA (asterisk in Fig. 3a) was also sequenced and found to contain a slightly shorter version of DmWRNexo starting from an internal methionine eight residues downstream from the initiator methionine.

As a negative control, a mock expression was conducted in the same *E. coli* strain transformed with the empty pIVEX2.3d vector, induced and harvested under identical conditions to wt DmWRNexo. This negative control bacterial lysate was applied to a His-trap column and fractions eluted and processed as for the recombinant his-tagged proteins; no appreciable protein bands were detected in these "peak" fractions (Fig. 3a bottom panel, lane "M" Fig. 3b).

DmWRNexo possesses 3′→5′ exonuclease activity

To assay possible nuclease activity of the recombinant DmWRNexo proteins, a 5′ fluorescein-end labelled oligonucleotide was annealed to complementary oligonucleotides to generate duplex templates with a 5′ overhang or blunt ends (see Table 1 for sequences). A single stranded 5′ fluorescein-labelled oligonucleotide was also used to determine if the proteins exhibited nuclease activity on single-stranded DNA. The recombinant DmWRNexo proteins were incubated with the various templates for 30 min then products analysed on denaturing acrylamide gels and visualised by excitation at 470 nm and emission at 520 nm. From Fig. 4a, it is apparent that wt DmWRN exo ("WT" in Fig. 4a) possesses exonuclease activity on both single stranded and 5′ overhang duplex templates, but has no activity against a blunt-ended template. Whilst 3′–5′ cleavage of the labelled oligonucleotide was observed in duplexes with either 5′ or 3′ overhangs (Fig. 4a and data not shown), no clipping of the 5′ terminal fluorescein was detected. These data, together with further analysis using other templates (data not shown), lead us to conclude that DmWRNexo possesses 3′–5′ exonuclease activity similar to human WRN. This is the first demonstration that the fly DmWRNexo protein is indeed an exonuclease.

To control for the possibility that the nuclease activity observed for wild type DmWRNexo may result from the presence of co-purifying *E. coli*

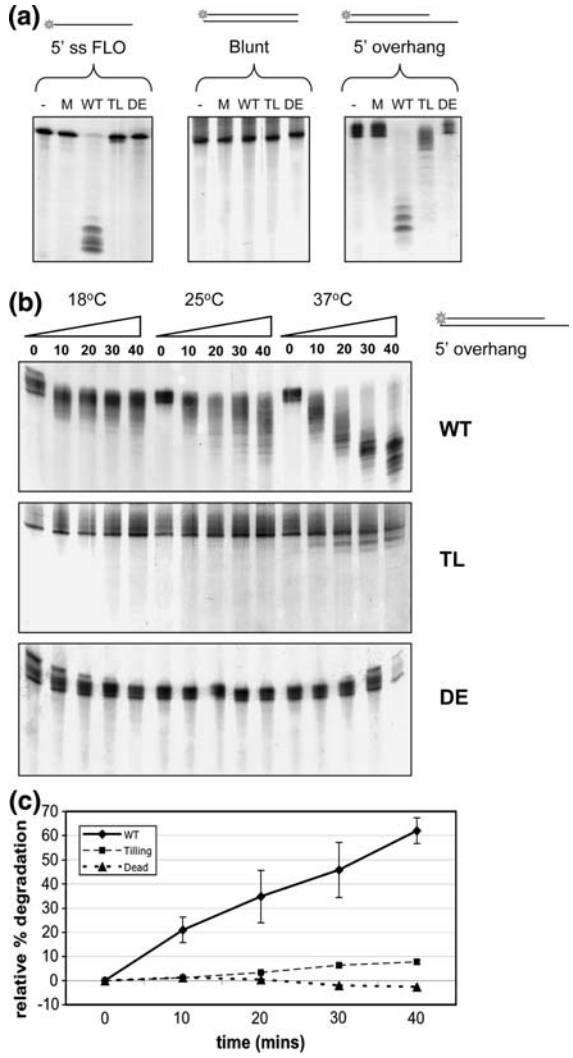

Fig. 4 Nuclease assays of DmWRNexo. Fluorescently 5′ end-labelled oligonucleotides were incubated with purified recombinant DmWRNexo and products analysed by denaturing acrylamide gel electrophoresis. **a** Activity of the various forms of DmWRNexo on various DNA substrates at 37°C for 30 min (see Table 1) for details of substrate sequences). **b** Impact of temperature on DmWRNexo exonuclease activity with time (in minutes, shown above each lane)− = buffer alone negative control, M = mock i.e. lysate from *E. coli* transformed with the empty vector, WT = wild type DmWRNexo, TL = DmWRNexo^{D229V} mutation ("TILLING"), DE = double mutant DmWRNexo^{D162A,E164A}. **c** Comparative nuclease activity on the 5′ overhang template at 37°C of wild type DmWRNexo (WT) versus the DmWRNexo^{D229V} mutation ("TILLING") and double mutant DmWRNexo^{D162A,E164A} ("Dead"), as quantitated from three independent experiments using ImageJ. *Error bars* are ±SEM

nucleases, the fractions from lysate of *E. coli* transformed with the empty pIVEX2.3d vector, equivalent to the peak fractions of wt DmWRNexo (See "M" in Fig. 3), were assayed for nuclease activity. It is clear from Fig. 4a that no nuclease activity on the assayed templates was present in these "mock" fractions ("M" in Fig. 4a), allowing us to conclude that any observed nuclease activity is dependant upon the presence of recombinant DmWRNexo.

Mutation decreases or ablates nuclease activity

The impact of the D229V mutation ("TL" in Fig. 4) on nuclease activity was analysed. Surprisingly for an amino acid change outside the presumed active site, DmWRNexo^{D229V} mutant protein showed little nuclease activity on the single stranded 5′ labelled template (left panel Fig. 4a), nor did it show any activity on blunt duplex DNA (middle panel Fig. 4a). Limited degradation of a duplex template with a 5′ overhang was observed, but the degree of degradation by DmWRNexo^{D229V} after 30 min at 37°C was far less than that observed for wild type DmWRNexo (compare WT and TL in right panel of Fig. 4a). DmWRNexo in which the presumptive active site residues D162 and E164 were mutated to alanine completely lacks exonuclease activity on single stranded or duplex templates (Fig. 4a, lanes "DE"), consistent with structural predictions that these represent active site residues important for metal ion co-ordination during catalysis (Perry et al. 2006; Saunders et al. 2008). Thus active site mutation completely abolished nuclease activity on the templates tested, while DmWRNexo^{D229V} protein has very limited 3′–5′ exonuclease activity.

Temperature dependence of DmWRNexo activity

Drosophila lab cultures are routinely maintained at 25°C, with viability of the CG7670^{e04496} homozygous mutant greater at 18°C (data not shown). We therefore tested the nuclease activity of DmWRNexo at these two temperatures in addition to 37°C, over a time course of 40 min. Limited activity of the wild type protein was detected at 18°C, with increased cleavage of the 5′ overhang template at 25°C and digestion to completion at 37°C after 40 min (Fig. 4b top panel). This is consistent with an enzyme optimum above 25°C. By contrast, essentially no cleavage of template was observed for DmWRNexo^{D229V} (TL in Fig. 4b) at either 18°C or 25°C. Moreover, only relatively large cleavage products were observed on exposure of the 5′ overhang substrate to the DmWRNexo^{D229V} mutant protein at 37°C, and there was no further increase after 20 min in either amount of cleavage product or a decrease in size of product with time (middle panel Fig. 4b), suggesting that this single point mutation results in an exonuclease with very poor processivity. As anticipated from the data in Fig. 4a, DmWRNexo in which two presumptive active site residues (D162, E164) are both mutated has no observable nuclease activity in these assays (bottom panel Fig. 4b). Simple quantification of relative exonuclease activity of wild type DmWRNexo and the mutant forms was calculated by taking the relative (compared to t_0) percentages of degraded compared to full-length substrate (Fig. 4c). This method may underestimate total activity as it ignores proportional calculation of sequential degradation of the same strand to produce shorter products. However, even using this relatively crude measure, wild type DmWRNexo can robustly turn over at least 6 × more substrate molecules than the DmWRNexo^{D229V} mutant over the same time frame at 37°C ($P = 0.00055$, Table 2). Under these conditions, the difference in activity between wild type DmWRNexo and the active site mutant DmWRNexo^{D162A,E164A} is also very significant, as is that between the active site mutant and DmWRNexo^{D229V} (Table 2). This analysis reinforces the results shown in Fig. 4a, b, in that wild type DmWRNexo possesses significant and processive exonuclease activity, whilst DmWRNexo^{D229V} has very little activity and the active site mutant DmWRNexo^{D162A,E164A} has essentially no activity under these experimental conditions.

Discussion

Werner syndrome provides a very useful model in which to study human ageing, but suffers from several drawbacks. Firstly, as it is a very rare syndrome, patient-derived material is limited in both quantity and cell type available. Genetic heterogeneity between patients represents a further challenge to analysis, and the presence of both helicase and

Table 2 Quantitative analysis of DmWRNexo exonuclease activity at 37°C

a

	Exp 1	Exp 2	Exp 3
WT	53.42	60.92	71.82
TL	8.64	6.17	8.44
DE	−1.60	−3.65	−2.63

b

t test pairs	*P*-value
WT–DE	2.74×10^{-4}
WT–TL	5.50×10^{-4}
TL–DE	4.68×10^{-4}

WT = wild type DmWRNexo; TL = DmWRNexo^{D229V} (TILLING mutation); DE = DmWRNexo^{D162A,E164A} (active site mutant). (a) Relative percentage of exonuclease activity; data from three independent experiments (exp). Note that these values are relative to the zero time point for each protein. For Image J quantification, the total signal was calculated as the sum of the signals from regions of the gel assigned as "uncut" and "degraded"; the proportion of degraded to total is shown above (part a) and in Fig. 4c. In nuclease-active samples (WT), the background "shadow" is lower due to rapid exonuclease activity; with little or no active nuclease (TL and DE), negative values arise from the higher amount of "shadow" at zero time. (b) Statistical analysis of these data: *P* values were calculated for pairwise comparisons using a 2-tailed student *t* test with $v = 2$

exonuclease activities on the same polypeptide makes interpretation of point mutation or RNAi experiments complex. We are therefore developing a fly model of Werner syndrome, since this allows a full dissection of the role of WRN through development of the organism, together with the ability to correlate phenotype in vivo with biochemical activity of the encoded protein in vitro. In invertebrates, as in bacteria (Courcelle and Hanawalt 1999) and plants (Hartung and Puchta 2006), we propose that the exonuclease and helicase activities of WRN are encoded on distinct genetic loci, enabling relatively easy genetic dissection of their roles. To this end, we have identified the *Drosophila* orthologue of the human exonuclease activity of WRN, encoded by the gene *CG7670*, and shown a hyperrecombinant phenotype in flies with a severe hypomorphic allele of *CG7670* in which very little mRNA is expressed due to piggyBac insertion into the 5′ UTR of the gene (Cox et al. 2007; Saunders et al. 2008). DmWRNexo, like WRN in higher eukaryotes, is therefore important in preventing excessive mitotic recombination that may arise as a consequence of DNA double strand breaks, for example at stalled replication forks (Rodriguez-Lopez et al. 2007). We are therefore now investigating how the WRN exonuclease suppresses or otherwise modulates mitotic recombination. Here, we have utilised TILLING to obtain a point mutation in *CG7670*, in an attempt to determine what features of DmWRNexo are important in its anti-recombinational role.

Interestingly, we find that flies heterozygous for *CG7670*^{D229V} and *CG7670*^{e04496} (*mwh*^{1} *CG7670*^{e04496}/*CG7670*^{D229V}) have elevated levels of recombination that are ~20-fold higher than background recombination in controls, although such recombination frequencies are dwarfed by those observed for the hypomorphic *CG7670*^{e04496} homozygotes, and even more so by flies hemizygous for *CG7670*^{e04496} (Fig. 1). These data strongly support the suggestion that DmWRNexo is limiting in flies with the piggyBac insertion in the *CG7670* gene, and that the degree of recombination is inversely related to the amount of DmWRNexo protein present: it probably acts stoichiometrically with DNA recombination substrates or intermediates in vivo. Interestingly, whilst the D229V mutant retains some ability to restrain excessive mitotic recombination, this is partially defective.

To understand why the D229V point mutation of DmWRNexo has an impact on DNA recombination, we turned to molecular modelling to identify the possible role of this amino acid in the protein. Such modelling (Fig. 2) suggests that aspartate 229 does not lie in proximity to the presumptive active site of the protein, but rather towards the outside of the molecule and is not predicted to be involved directly in exonuclease catalysis. On spatial rotation of this model (data not shown) it appears that aspartate 229 may lie in a cleft within the protein, and it is conceivable that this may play a role in modulating exonuclease activity, perhaps through mediating association either with the DNA template or with proteins that may bind to DmWRNexo.

To determine if the increased rates of recombination observed in flies with the *CG7670*^{D229V} mutation might arise from decreased exonuclease activity of DmWRNexo^{D229V}, or some other factor such as loss of a protein interaction site, we developed a novel fluorescence-based platform for conducting WRN

exonuclease assays, which may be adaptable to higher throughput assays. Importantly, we show for the first time that DmWRNexo does have exonuclease activity on both single stranded and duplex templates bearing overhangs (but not blunt ended duplex DNA), and moreover that it cleaves in a 3′→5′ direction, as reported for human WRN (Huang et al. 1998). Furthermore, mutation of acidic amino acids D162 and E164 to alanine, equivalent to the catalytically critical metal–ion coordinating residues in human WRN, ablates all exonuclease activity, further strengthening the similarity with human WRN. Interestingly, recombinant DmWRNexo bearing the D229V mutation showed very limited exonuclease activity on a 5′ overhang substrate but absolutely no activity was detectable against single stranded DNA. Moreover, the small amount of cleavage detected with this mutant enzyme did not increase with time, and was only detectable at 37°C, a non-physiological temperature for flies, though it is important to note that in the wild, fly larvae will often unavoidably experience relatively high temperatures, although not often over 37°C for sustained periods. It is possible that whilst flies are maintained at 25°C in the lab, DmWRNexo optimum is higher than this—many mammalian enzymes have increased turnover rates at temperatures above physiological until they begin to denature and lose activity. In terms of the exonuclease assay, it is also conceivable that greater "breathing" of duplex DNA will occur at 37°C compared with 25°C, allowing access to single stranded DNA ends for enzyme binding: however, the results using a blunt duplex template at 37°C (Fig. 4a) do not support this assertion.

We can only speculate at this stage on why mutation of amino acid aspartate 229, distant from the active site, has such a marked impact on exonuclease activity. Alteration of the charged aspartate 229 on the protein surface to a non-polar valine residue may impact significantly on the folding or stability of the protein in vitro, while protein interactions around this site in vivo may act to stabilize the mutant form, accounting for the low nuclease activity in vitro but the mild phenotype in flies. Alternatively, it is possible that the DNA substrate loops over this region of the protein prior to entering the active site and that changes in surface charge of the protein negatively impact on such interactions—perhaps a duplex template interacts more stably than a single stranded template on the altered protein surface. The low processivity of the DmWRNexo^{D229V} mutant enzyme suggests that DNA-protein association may be important: it is highly possible that the substrate simply dissociates from the D229V mutant form of the enzyme after cleavage of a few nucleotides, because association is too weak. These speculations await experimental confirmation in the form of DNA-enzyme co-crystals, or structural investigation by sensitive techniques such as NMR. What must also be considered is the severe loss of nuclease activity in vitro of the D229V mutant enzyme, compared with a relatively mild recombination phenotype in vivo for flies with the *CG7670*^{e04496}/*CG7670*^{D229V} genotype. From the results in Fig. 1a, b, it is clear that DmWRNexo protein is limiting in *CG7670*^{e04496} homozygotes, such that recombination rates (single cell clones with *mwh* phenotype) approximately double when the gene dosage halves. We assume that mutation of the D229 residue does not impact on levels of protein expression, so that although flies with the mutation may have little exonuclease activity per molecule, they will have appreciable amounts of the enzyme. It is therefore possible that there is still sufficient residual exonuclease activity for excessive Holliday junction-dependent recombination to be suppressed (see Rodriguez-Lopez et al. 2007). Additionally, it is highly likely that DmWRNexo does not operate in isolation within the nucleus, and that it is part of a large multiprotein recombination and/or replication complex, as shown for human WRN (Lebel et al. 1999). It is possible that in modulating recombination, DmWRNexo's most important role is recruitment of other factors, such as RecQ helicases (e.g. DmBLM, encoded by *mus309* (McVey et al. 2007)), rather than exonuclease activity per se. We are therefore currently analyzing DNA recombination involving *Drosophila* RecQ helicases. In conclusion, using tagged recombinant DmWRNexo, we have shown for the first time that DmWRNexo possesses 3′–5′ exonuclease activity, and generated an active site mutant version of the enzyme which lacks nuclease activity. In addition, we have correlated increased mitotic recombination in flies bearing a single D229V mutation in DmWRNexo with a large reduction in nuclease activity in vitro. These data strongly support the importance of DmWRNexo in suppressing genomic instability in flies.

Acknowledgments We thank Christine Borer for technical support, and Tony Willis for protein sequencing. This work was supported by the Biotechnology and Biological Sciences Research Council [grant numbers BB/E000924/1, BB/E002072/1 and BB/E016995/1].

References

Cheng WH, Muftuoglu M, Bohr VA (2007) Werner syndrome protein: functions in the response to DNA damage and replication stress in S-phase. Exp Gerontol 42:871–878. doi:10.1016/j.exger.2007.04.011

Courcelle J, Hanawalt PC (1999) RecQ and RecJ process blocked replication forks prior to the resumption of replication in UV-irradiated *Escherichia coli*. Mol Gen Genet 262:543–551. doi:10.1007/s004380051116

Cox LS, Faragher RG (2007) From old organisms to new molecules: integrative biology and therapeutic targets in accelerated human ageing. Cell Mol Life Sci 64:2620–2641. doi:10.1007/s00018-007-7123-x

Cox LS, Clancy DJ, Boubriak I, Saunders RD (2007) Modeling Werner Syndrome in *Drosophila melanogaster*: hyper-recombination in flies lacking WRN-like exonuclease. Ann N Y Acad Sci 1119:274–288. doi:10.1196/annals.1404.009

Davis T, Baird DM, Haughton MF, Jones CJ, Kipling D (2005) Prevention of accelerated cell aging in Werner syndrome using a p38 mitogen-activated protein kinase inhibitor. J Gerontol A Biol Sci Med Sci 60:1386–1393

Dhillon KK, Sidorova J, Saintigny Y, Poot M, Gollahon K, Rabinovitch PS, Monnat RJ Jr (2007) Functional role of the Werner syndrome RecQ helicase in human fibroblasts. Aging Cell 6:53–61. doi:10.1111/j.1474-9726.2006.00260.x

Faragher RG, Kill IR, Hunter JA, Pope FM, Tannock C, Shall S (1993) The gene responsible for Werner syndrome may be a cell division "counting" gene. Proc Natl Acad Sci USA 90:12030–12034. doi:10.1073/pnas.90.24.12030

Hartung F, Puchta H (2006) The RecQ gene family in plants. J Plant Physiol 163(3):287–296. doi:10.1016/j.jplph.2005.10.013

Hayflick L (1965) The limited in vitro lifetime of human diploid cell strains. Exp Cell Res 37:614–636. doi:10.1016/0014-4827(65)90211-9

Huang S, Li B, Gray MD, Oshima J, Mian IS, Campisi J (1998) The premature ageing syndrome protein, WRN, is a 3′→5′ exonuclease. Nat Genet 20:114–116. doi:10.1038/2410

Lawrence P, Johnston P, Morata G (1986) Methods of marking cells. In: Roberts DB (ed) *Drosophila*: a practical approach. IRL, Oxford, pp 229–242

Lebel M, Spillare EA, Harris CC, Leder P (1999) The Werner syndrome gene product co-purifies with the DNA replication complex and interacts with PCNA and topoisomerase I. J Biol Chem 274(53):37795–37799. doi:10.1074/jbc.274.53.37795

McCallum CM, Comai L, Greene EA, Henikoff S (2000) Targeting induced local lesions IN genomes (TILLING) for plant functional genomics. Plant Physiol 123:439–442. doi:10.1104/pp.123.2.439

McVey M, Andersen SL, Broze Y, Sekelsky J (2007) Multiple functions of *Drosophila* BLM helicase in maintenance of genome stability. Genetics 176:1979–1992. doi:10.1534/genetics.106.070052

Opresko PL, Laine JP, Brosh RM Jr, Seidman MM, Bohr VA (2001) Coordinate action of the helicase and 3′ to 5′ exonuclease of Werner syndrome protein. J Biol Chem 276:44677–44687. doi:10.1074/jbc.M107548200

Peitsch MC, Herzyk P, Wells TN, Hubbard RE (1996) Automated modelling of the transmembrane region of G-protein coupled receptor by Swiss-model. Receptors Channels 4:161–164

Perry JJ, Yannone SM, Holden LG, Hitomi C, Asaithamby A, Han S, Cooper PK, Chen DJ, Tainer JA (2006) WRN exonuclease structure and molecular mechanism imply an editing role in DNA end processing. Nat Struct Mol Biol 13:414–422. doi:10.1038/nsmb1088

Rodriguez-Lopez AM, Jackson DA, Iborra F, Cox LS (2002) Asymmetry of DNA replication fork progression in Werner's syndrome. Aging Cell 1:30–39. doi:10.1046/j.1474-9728.2002.00002.x

Rodriguez-Lopez AM, Whitby MC, Borer CM, Bachler MA, Cox LS (2007) Correction of proliferation and drug sensitivity defects in the progeroid Werner's syndrome by Holliday junction resolution. Rejuvenation Res 10:27–40. doi:10.1089/rej.2006.0503

Salk D, Au K, Hoehn H, Stenchever MR, Martin GM (1981) Evidence of clonal attenuation, clonal succession, and clonal expansion in mass cultures of aging Werner's syndrome skin fibroblasts. Cytogenet Cell Genet 30:108–117. doi:10.1159/000131597

Saunders RD, Boubriak I, Clancy DJ, Cox LS (2008) Identification and characterization of a *Drosophila* ortholog of WRN exonuclease that is required to maintain genome integrity. Aging Cell 7:418–425. doi:10.1111/j.1474-9726.2008.00388.x

Schwede T, Kopp J, Guex N, Peitsch MC (2003) SWISS-MODEL: An automated protein homology-modeling server. Nucleic Acids Res 31:3381–3385. doi:10.1093/nar/gkg520

Sidorova JM, Li N, Folch A, Monnat RJ Jr (2008) The RecQ helicase WRN is required for normal replication fork progression after DNA damage or replication fork arrest. Cell Cycle 7:796–807

Till BJ, Colbert T, Tompa R, Enns LC, Codomo CA, Johnson JE, Reynolds SH, Henikoff JG, Greene EA, Steine MN, Comai L, Henikoff S (2003) High-throughput TILLING for functional genomics. Methods Mol Biol 236:205–220

Yu CE, Oshima J, Fu YH, Wijsman EM, Hisama F, Alisch R, Matthews S, Nakura J, Miki T, Ouais S, Martin GM, Mulligan J, Schellenberg GD (1996) Positional cloning of the Werner's syndrome gene. Science 272:258–262. doi:10.1126/science.272.5259.258

Yu CE, Oshima J, Wijsman EM, Nakura J, Miki T, Piussan C, Matthews S, Fu YH, Mulligan J, Martin GM, Schellenberg GD (1997) Mutations in the consensus helicase domains of the Werner syndrome gene. Werner's syndrome collaborative group. Am J Hum Genet 60:330–341